INSTITUTE OF PHYSICS PUBLISHING JOURNAL OF PHYSICS B: ATOMIC, MOLECULAR AND OPTICAL PHYSICS

J. Phys. B: At. Mol. Opt. Phys. **37** (2004) 2379–2385 PII: S0953-4075(04)75861-7

Coupled mean-field description of electron removal processes in He^+–Ne and He^+–Ar collisions

T Kirchner[1], **M Horbatsch**[2] **and H J Lüdde**[3]

[1] Institut für Theoretische Physik, TU Clausthal, Leibnizstraße 10, D-38678 Clausthal-Zellerfeld, Germany
[2] Department of Physics and Astronomy, York University, Toronto, Ontario, M3J 1P3, Canada
[3] Institut für Theoretische Physik, Johann Wolfgang Goethe-Universität, Robert-Mayer-Straße 8, D-60054 Frankfurt/Main, Germany

E-mail: tom.kirchner@tu-clausthal.de

Received 7 February 2004
Published 17 May 2004
Online at stacks.iop.org/JPhysB/37/2379
DOI: 10.1088/0953-4075/37/11/014

Abstract

Ion–atom collisions with active projectile and target electrons are considered in an approach which combines mean-field models for both types of electrons. A previous calculation is improved by taking into account the nonorthogonality of the propagated orbitals. Results for net recoil ion and free electron production in He^+–Ne and He^+–Ar collisions are shown to be in good agreement with experiments.

Ion–atom collisions with active electrons on both nuclei have been of interest experimentally and theoretically [1–5], as they are of practical relevance in plasmas [6], planetary aurorae [7] and accelerator technology [8]. Moreover, they represent fundamentally important few-body systems which exhibit interesting electron dynamics at collision energies where electron removal occurs. In this region, perturbative methods are questionable and one is faced, in principle, with a correlated many-electron problem whose explicit solution cannot yet be implemented if more than two electrons are active. Thus, a mean-field description treating all electrons as indistinguishable is desirable. In the framework of the semiclassical approximation in which one assumes that the heavy particles move on classical (straight-line) trajectories, such approaches are readily formulated on the level of time-dependent Hartree Fock (TDHF) [9] or time-dependent density functional theory (TDDFT) [10, 11]. In practice, however, they are limited to systems of electrons bound initially to one centre only [12–14].

In a recent work [3], we have addressed the He^+–Ne collision system from a simplified viewpoint based on different mean-field descriptions for the initial projectile and target electrons. The target electrons were propagated in a single-particle potential made up of the following additive components: the atomic ground state potential of Ne, a global time-dependent screening potential due to the partial electron removal and the Coulomb potential

of the projectile nucleus screened by the potential of a frozen $He^+(1s)$ electron. The projectile electron was propagated in the Coulomb potential of its parent nucleus and the exponentially decreasing potential of the neutral Ne atom, moving on a classical trajectory in the projectile reference frame. The transition amplitudes of both sets of calculations were then combined statistically to calculate total cross sections for various charge-changing processes.

While the overall agreement with experimental data was encouraging, some discrepancies were observed, most notably for the net recoil ion production cross section which measures the average charge state of the recoiling target ion. We proposed that a more refined dynamical screening model would be necessary to explain the data at impact energies below $E_P = 30$ keV/amu, but we could not corroborate this suggestion by calculations. Furthermore, we could not exclude the possibility that our combination of mean-field descriptions was too simplistic, or that perhaps electron correlation effects might be important which are omitted in present mean-field approaches.

Here we demonstrate that the situation is not as complicated as the above caveat might suggest: it is not necessary to refine the dynamical screening model itself in order to obtain good agreement with experiment for the net recoil ion production cross section down to a few keV/amu. We apply the same procedure as before to evolve the single-particle orbitals, but we improve the model by accounting for the nonorthogonality of the time-developed projectile and target orbitals in the final-state analysis. The nonorthogonality is due to the use of different Hamiltonians for the propagation of the projectile and target orbitals and does not occur in a single mean-field approach such as TDHF or TDDFT. We find a significant improvement for the recoil ion production cross section and also good agreement with experiments for the free electron production cross section.

In order to test the validity of the proposed coupled mean-field independent electron model, we have also considered the He^+–Ar scattering system for which no prior theoretical analysis of these net cross sections was available. The findings are qualitatively similar to the He^+–Ne data. Since the outer shells of Ne and Ar have rather different properties, one can conclude that the present findings are applicable for a wide class of ion–atom collisions.

The procedure should also be of interest for more general situations involving fermions which belong to different systems initially, but lose their distinguishability during a dynamical process. We focus on an accurate description of net electron cross sections since they depend directly on the overall electron density, and thus should be amenable to a treatment by TDDFT. The present findings should have implications for other fields: TDDFT is being currently applied to collisions involving atomic clusters [15], and related mean-field models have been applied to nuclear collision problems [16].

We have solved the single-particle equations for projectile and target electrons using the same implementation of the basis generator method (BGM) [17] as in our previous works for collisions with Ne [3] and Ar [18]. The BGM consists of a coupled-channel representation of the time-dependent orbitals in a dynamically adapted basis. We have also calculated the overlap integrals $S_{ij}(t_f) = \langle \psi_i(t_f) | \psi_j(t_f) \rangle$ for the propagated projectile and target states at the final time $t = t_f$ chosen such that the distance between the projectile and target nuclei is 40 au. This choice guarantees convergence of our results to within 1%. We found that the $S_{ij}(t_f)$ are largest at low collision energies where their absolute squares reach values of up to 0.3. In this region electron transfer channels are strong; i.e. both initial projectile and target electrons populate states of the other nucleus after the collision. At higher impact energies, ionization dominates and the geometrical overlap is small. Moreover, contributions that are associated with transfer to the other centre are augmented by translation factors whose oscillatory patterns produce orthogonality even for states that overlap significantly in configuration space.

In order to take into account the nonorthogonality of orbitals in the final-state analysis for the system of $N = N_T + N_P$ target and projectile electrons, we assume that the N-electron wavefunction Ψ is given at $t = t_f$ as a determinant of the propagated spin orbitals $\phi_j(x, t_f) = \psi_j(\mathbf{r}, t_f)\chi_{\sigma_j}(s)$ with spatial parts $\psi_j(\mathbf{r}, t_f)$ and standard spin functions $\chi_{\sigma_j}(s)$

$$\Psi(x_1, \ldots, x_N; t_f) = \frac{\det(\phi_1(x_1, t_f), \ldots, \phi_N(x_N, t_f))}{\sqrt{N!\det(S_{11}(t_f), \ldots, S_{NN}(t_f))}}. \tag{1}$$

The factor in the denominator ensures normalization despite the nonvanishing overlap integrals $S_{ij}(t_f)$, i.e.

$$\langle\Psi(t_f)|\Psi(t_f)\rangle = 1. \tag{2}$$

The corresponding one-particle density

$$n(\mathbf{r}, t_f) = N \sum_{s_1,\ldots,s_N} \int |\Psi(\mathbf{r}, s_1, x_2, \ldots, x_N; t_f)|^2 \, \mathrm{d}^3 r_2, \ldots, \mathrm{d}^3 r_N, \tag{3}$$

cannot be reduced to a simple sum of orbital densities, but using Cramer's rule one can show that equation (3) equals the expression

$$n(\mathbf{r}, t_f) = \sum_{i,j=1}^{N} S_{ij}^{-1}(t_f)\psi_j^*(\mathbf{r}, t_f)\psi_i(\mathbf{r}, t_f), \tag{4}$$

which involves matrix elements of the inverse overlap matrix. Equations (1) and (4) are valid for any set of nonorthonormal orbitals. In our case, each orbital is normalized due to its unitary time development and only overlap integrals that involve both a propagated target and the propagated projectile orbital are nonzero.

The average electron numbers (the so-called net probabilities) of present interest are given as integrals of the density over regions in configuration space that correspond to bound target, bound projectile and continuum states [11]. As a consequence of equation (4) they also carry information on the overlap of orbitals. Instead of performing these integrations in r-space we use a channel representation, in which the different contributions are characterized by finite sets of single-particle states. This procedure is better adapted to the BGM. The average number of electrons in target (T) and projectile (P) are then given by

$$P_{\mathrm{net}}^{\mathrm{T,P}} = \sum_{i,j=1}^{N} \sum_{k=1}^{K_T, K_P} c_k^{i(\mathrm{T,P})} S_{ij}^{-1} c_k^{j*(\mathrm{T,P})} \Big|_{t=t_f}, \tag{5}$$

with single-particle amplitudes for populating the set of bound target and projectile states $\left\{\left|\varphi_k^{(\mathrm{T,P})}\right\rangle, k = 1, \ldots, K_T, K_P\right\}$

$$c_k^{i(\mathrm{T,P})} = \left\langle\varphi_k^{(\mathrm{T,P})} \,\middle|\, \psi_i\right\rangle\Big|_{t=t_f}. \tag{6}$$

Note that $N = N_T + N_P$ is the number of electrons, while K_T and K_P represent the number of bound states at target and projectile incorporated explicitly in the BGM calculation. With $K_{T,P} > N_{T,P}$ one describes bound-state excitations. Net recoil ion production $P_{\mathrm{net}}^{\mathrm{rec}}$ and net free electron production $P_{\mathrm{net}}^{\mathrm{free}}$ are calculated according to

$$P_{\mathrm{net}}^{\mathrm{rec}} = N_T - P_{\mathrm{net}}^{\mathrm{T}}, \tag{7}$$

$$P_{\mathrm{net}}^{\mathrm{free}} = N - P_{\mathrm{net}}^{\mathrm{T}} - P_{\mathrm{net}}^{\mathrm{P}}, \tag{8}$$

and are integrated over the impact parameter to obtain total cross sections.

In figure 1, we show the net recoil ion production cross section for He^+–Ne collisions. We compare four sets of calculations with experimental data: results obtained in the so-called

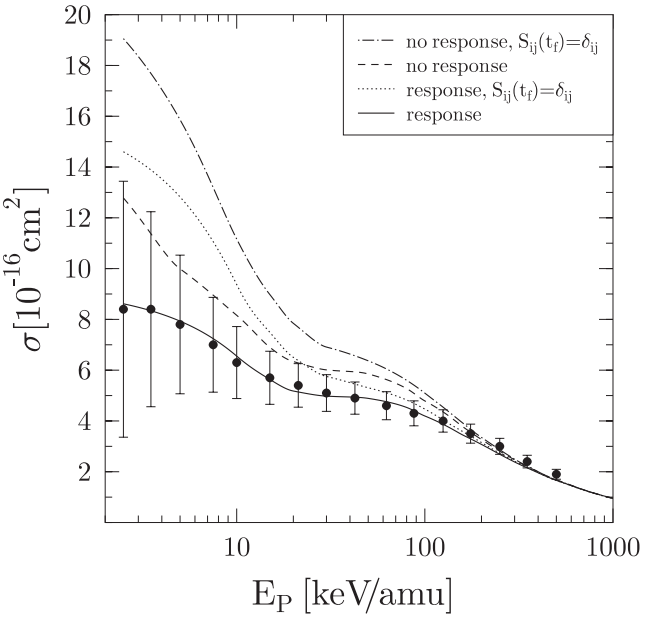

Figure 1. Total cross section for net recoil ion production as a function of impact energy for He^+–Ne collisions. Lines: present theoretical results; lines labelled $S_{ij}(t_f) = \delta_{ij}$: previous results from [3]. Symbols: experimental data from [19].

no-response approximation, in which the dynamical screening potential in the Hamiltonian for the initial target electrons is neglected, results that include the dynamical screening potential (response), as well as our previous no-response and response results [3], in which the nonorthogonality problem was ignored (i.e. it was *assumed* in equations (7) and (8) that $S_{ij}(t_f) = \delta_{ij}$).

At high impact energies, the results of all sets of calculations merge and are in good agreement with the experimental data. This demonstrates that neither response nor nonorthogonality effects are important in fast collisions, in which ionization processes dominate and where the short interaction time prevents them to be sensitive to time-dependent changes of the electronic interaction. This changes decisively towards lower impact energies where electron transfer becomes more important. Both response and nonorthogonality effects reduce the cross section, and very good agreement with experiment down to the lowest energies considered is obtained if we take both of them into account. The reduction of electron removal cross sections due to response has been observed in many previous studies (see, e.g., [3, 18]). It reflects the fact that the dynamical screening potential that we employ is attractive and increases the binding of the target electrons. The nonorthogonality effect is more subtle: the details of the calculations show that the overlap integrals $S_{ij}(t_f)$ become appreciable when electrons are captured to the projectile with significant probabilities and occupy the same states (mainly 1s) as the initial projectile electron. This leads to an overcounting of the population of bound projectile states which is corrected once the total probability is renormalized appropriately by including the inverse overlap matrix in the evaluation of $P_{\mathrm{net}}^{\mathrm{rec}}$ [cf equation (5)].

In figure 2, we show similar results for net free electron production. In this case, our previous no-response and response results are within the experimental error bars. Inclusion of the overlaps via equation (5) increases the cross section at low and intermediate impact energies because the overcounting of electrons in bound projectile states is partly compensated

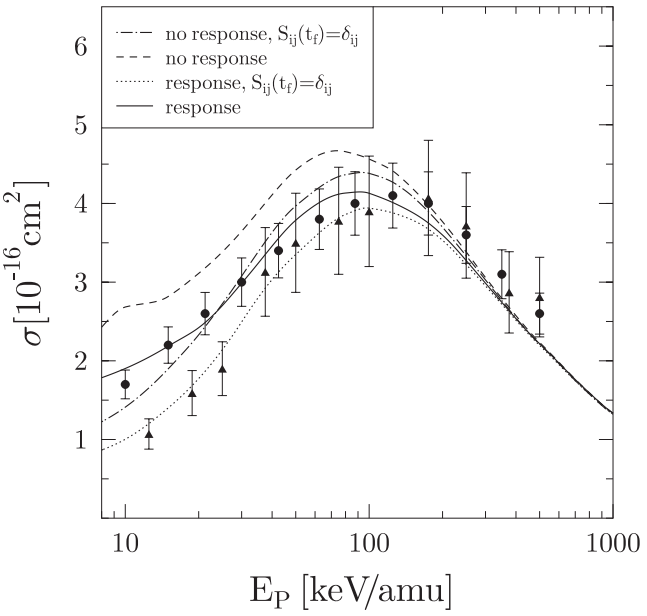

Figure 2. Total cross section for net free electron production as a function of impact energy for He^+–Ne collisions. Lines: present theoretical results; lines labelled $S_{ij}(t_f) = \delta_{ij}$: previous results from [3]. Symbols: experimental data from [19] (circles) and [20] (triangles).

by continuum channels. Only if response effects are also taken into account do the results remain within the experimental error bars, except for the lowest impact energies where the theoretical cross section is still too high and appears to have a wrong slope.

In this region, it becomes increasingly difficult to separate the relatively small continuum contribution from the larger contribution due to electron capture to the projectile, as the populated continuum states have significant probability density concentrated near the projectile nucleus. In particular, we find small but non-negligible continuum contributions at relatively large impact parameters $b > 2$ au which are wrongfully enhanced if they are convolved with the inverse overlap matrix according to equation (5). This problem becomes severe at energies below $E_P = 10$ keV/amu where the overlaps of the propagated target and projectile orbitals reach their highest values. As the results for free electron production obtained in this region are clearly in error, we are showing only results from 8 keV/amu in figure 2. We note that the comparably large electron capture cross section is not significantly affected by these problems. This channel cannot be computed directly from the overall electron density (4) as it corresponds to a particular final charge state of one of the collision partners. Rather, the final N-electron wavefunction (1) itself has to be analysed, which can be done by using the concept of *inclusive probabilities* [21, 22], but which is beyond the scope of the present paper.

Figures 3 and 4 display analogous results for these net cross sections for Ar target atoms. Again, the net recoil ion production cross section (figure 3) is in very good agreement with experiment once response and nonorthogonality effects are both taken into account. We observe some structures in the calculations around $E_P = 15$ keV/amu, which are neither supported nor contradicted by the measured data due to their relatively large uncertainty. In the case of the free electron production cross section (figure 4), we find good agreement with experiments down to $E_P = 10$ keV/amu. For even lower impact energies we could not separate the ionization contribution from the contribution due to electron capture with sufficient accuracy for the same reasons as discussed above for Ne targets.

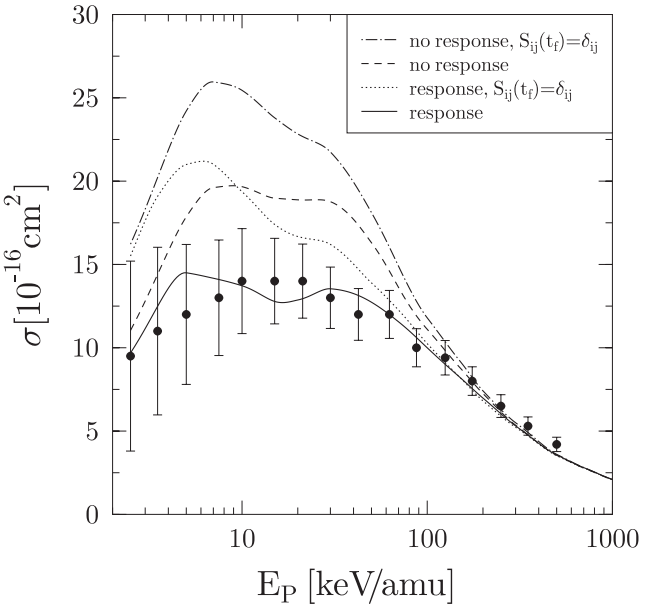

Figure 3. Total cross section for net recoil ion production as a function of impact energy for He^+–Ar collisions. Lines: present theoretical results. Symbols: experimental data from [19].

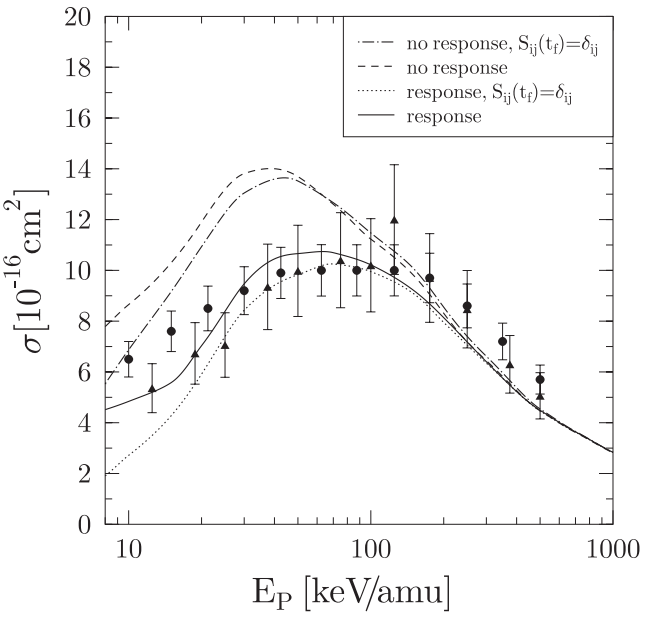

Figure 4. Total cross section for net free electron production as a function of impact energy for He^+–Ar collisions. Lines: present theoretical results. Symbols: experimental data from [19] (circles) and [20] (triangles).

Similarly to previously investigated bare-ion collisions with Ar atoms [18], we find substantial target excitation probabilities at low and intermediate impact energies which might contribute to the recoil ion and free electron production cross sections via autoionization (AI)

of multiply excited states. In [18], we applied a simple model based on multinomial statistics to obtain an upper estimate for these contributions, and found a 10–15% increase of the net recoil ion production cross sections below collision energies $E_P \approx 50$ keV/amu and an enhancement of free electron production of up to 100% at the lowest impact energies where direct ionization is weak. The magnitude of these enhancements due to AI appears to be highly overestimated by the simple multinomial analysis. Moreover, the model used is too simplistic for the present collision system, in which nonorthogonality effects occur. Therefore, we have not considered AI in figures 3 and 4, but we emphasize that an independent investigation of the magnitude of AI processes in low-energy collisions with Ar atoms would be desirable to clarify this issue.

In conclusion, we find that a satisfactory description of net recoil ion production, as well as free electron production in He^+ collisions with Ne and Ar atoms can be obtained by a coupled mean-field theory which is corrected for the lack of orthogonality of projectile and target orbitals caused by the propagation with different single-particle Hamiltonians. At the lowest energies considered (below 15 keV/amu for Ne and 10 keV/amu for Ar), some issues remain outstanding with respect to the free electron production. These are most likely caused by the difficulty of separating projectile bound-state contributions from the continuum, which is predominantly represented by projectile continuum states at these energies.

Acknowledgments

This work was supported by the Deutsche Forschungsgemeinschaft and the Natural Sciences and Engineering Research Council of Canada.

References

[1] Montenegro E C, Meyerhof W E and McGuire J H 1994 *Adv. At. Mol. Opt. Phys.* **34** 249
[2] Cocke C L and Montenegro E C 1996 *Comments At. Mol. Phys.* **32** 131
[3] Kirchner T and Horbatsch M 2001 *Phys. Rev.* A **63** 062718
[4] Montenegro E, Santos A C F, Melo W S, Sant'Anna M M and Sigaud G M 2002 *Phys. Rev. Lett.* **88** 013201
[5] Montanari C, Miraglia J and Arista N 2003 *Phys. Rev.* A **67** 062702
[6] Yoon J S and Jung Y D 1999 *Phys. Plasmas* **6** 3391
[7] Liu W H and Schultz D R 2000 *Astrophys. J.* **530** 500
[8] Kaminskii A K and Vasil'ev A A 1998 *Phys. Part. Nucl.* **29** 201
[9] Blaizot J P and Ripka G 1986 *Quantum Theory of Finite Systems* (Cambridge, MA: MIT Press) ch 9
[10] Gross E K U, Dobson J F and Petersilka M 1996 *Topics in Current Chemistry* vol 181 ed R F Nalewajski (Heidelberg: Springer) p 81
[11] Lüdde H J 2003 *Many-Particle Quantum Dynamics in Atomic and Molecular Fragmentation* ed J Ullrich and V P Shevelko (Heidelberg: Springer) p 205
[12] Nagano R, Yabana K, Tazawa T and Abe Y 2000 *Phys. Rev.* A **62** 062721
[13] Tong X M, Watanabe T, Kato D and Ohtani S 2002 *Phys. Rev.* A **66** 032709
[14] Keim M, Achenbach A, Lüdde H J and Kirchner T 2003 *Phys. Rev.* A **67** 062711
[15] Calvayrac F, Reinhardt P G, Suraud E and Ullrich C A 2000 *Phys. Rep.* **337** 493
[16] Bonasera A, Gulminelli F and Molitoris J 1994 *Phys. Rep.* **243** 1
[17] Kroneisen O J, Lüdde H J, Kirchner T and Dreizler R M 1999 *J. Phys. A: Math. Gen.* **32** 2141
[18] Kirchner T, Horbatsch M and Lüdde H J 2002 *Phys. Rev.* A **66** 052719
[19] Rudd M E, Goffe T V, Itoh A and DuBois R D 1985 *Phys. Rev.* A **32** 829
[20] DuBois R D 1989 *Phys. Rev.* A **39** 4440
[21] Lüdde H J and Dreizler R M 1985 *J. Phys. B: At. Mol. Phys.* **18** 107
[22] Kirchner T, Lüdde H J and Horbatsch M 2004 *Phys. Scr.* at press